

Modeling of Mass Transport into Immiscible Polymeric Blends

Ali El Afif,^{*,†} Ricardo Cortez,[†] Donald P. Gaver III,[‡] and Daniel de Kee[§]*Mathematics Department, Biomedical Engineering Department, and Chemical Engineering Department, Center for Computational Science, Tulane University, New Orleans, Louisiana 70118**Received February 21, 2003; Revised Manuscript Received September 13, 2003*

ABSTRACT: A nonlinear 3D model for mass transport into immiscible polymeric blends is developed by explicitly incorporating the interface dynamics into the transport equations. The interface is characterized, on a mesoscopic level of description, by a scalar $Q(\mathbf{r}, t)$ and a second-order tensor $\mathbf{q}(\mathbf{r}, t)$ respectively describing the local size and anisotropy densities of the interfacial area. The newly obtained constitutive equation for the diffusion mass flux density extends Fick's first law by involving two additional terms accounting for the local changes of the interface morphology. The model provides an expression for the distribution of both isotropic (Laplace) and anisotropic stresses created by mass transport within the immiscible polymeric blend. The governing equations are parametrized by the free energy density that includes a mixing part and an excess energy term attributed to the presence of the interface. We investigate in more detail a one-dimensional sorption process of a solvent into a thin immiscible blend consisting of a matrix and a dispersed phase. Three dimensionless groups of physical parameters arise in the 1D dimensionless formulation; two are coupling constants that explicitly relate diffusion to the interface dynamic changes, and one is the diffusion Deborah number. Numerical results show that diffusion becomes non-Fickian for values of Deborah number approaching unity. The time evolution of the calculated mass uptake, swelling, stresses, and total size and anisotropy densities provides a good indication of the effects of diffusion–interface interaction on both mass transport and the morphology of the interface.

I. Introduction

Mass transport of low molecular weight substances into polymeric materials is an important process in many areas of today's application. Examples include protective coatings, drug delivery systems, and bio-science. Since the vast majority of polymers are naturally immiscible, there is a growing interest for the use of such immiscible systems in the design and manufacture of materials with tailored morphologies possessing properties unavailable with their homopolymer counterparts. One obvious manifestation of immiscibility is the presence of an interface that separates the different components. The interface, characterized by its size and shape, plays a key role in determining the physical as well as the mechanical properties of immiscible blends. The size and shape of the interface are determined by the competition among many factors, the most important of which are identified to be the flow field, the interfacial tension, and the probable presence of inclusions.

Although diffusion is a ubiquitous process in most multicomponent immiscible mixtures involving small molecules, it has not received enough attention. Currently, most investigations devoted to the dynamics of immiscible polymeric blends are rheological. Such studies focus on understanding the effects of an applied flow on the interface morphology that, in most cases, undergoes significant changes as a result of the occurrence of simultaneous and concomitant coalescence and break-up processes produced by interfacial distortions/deformations. These mechanical changes, attributed mainly to the *interface–flow* interaction, create isotropic as well

as anisotropic stresses that generally subsist within the blend after cessation of the external flow. Here, we study a different dynamic phenomenon that is related to the isothermal unsteady mass transport of a solvent into an immiscible polymeric blend. It consists of investigating the *interface–diffusion* interaction, in the absence of an external flow and under mechanical equilibrium. In other words, this paper is devoted to elucidate the effects of the coupling arising between diffusion and the deformation of the interface on both the process of mass transport as well as on the morphology of the interface.

It is well-known that mass transport into complex media is generally accompanied by the creation of internal stresses resulting from local deformations (e.g., swelling) of the internal structure. These structural changes strongly influence the transport behavior whose dynamics is beyond the range of predictions of Fick's linear theory.^{1–10} Therefore, to appropriately describe non-Fickian manifestations, it is of primordial importance to identify the nature of the internal structure and how its dynamics couples to diffusion. Here, our structured system is a blend of immiscible polymers that embeds an interface. The morphology of the interface may be as simple as that observed in media consisting of a matrix and a dispersed phase with a spherical symmetry or as complex as that observed in co-continuous media. We seek to describe diffusion on a more microscopic level than that provided by the classical Fickian theory. Indeed, whereas the latter is based on the use of one independent state variable, namely the concentration of penetrants, our approach involves extra internal variables that directly track the interfacial changes produced by the diffusion mass fluxes. Thereby, this mesoscopic description allows us to gain more information concerning the interface–diffusion interaction by utilizing two structural variables defined as moments of an interfacial kinetic distribution function.¹¹

[†] Mathematics Department.

[‡] Biomedical Engineering Department.

[§] Chemical Engineering Department.

* Corresponding author: e-mail alielif@hotmail.com.

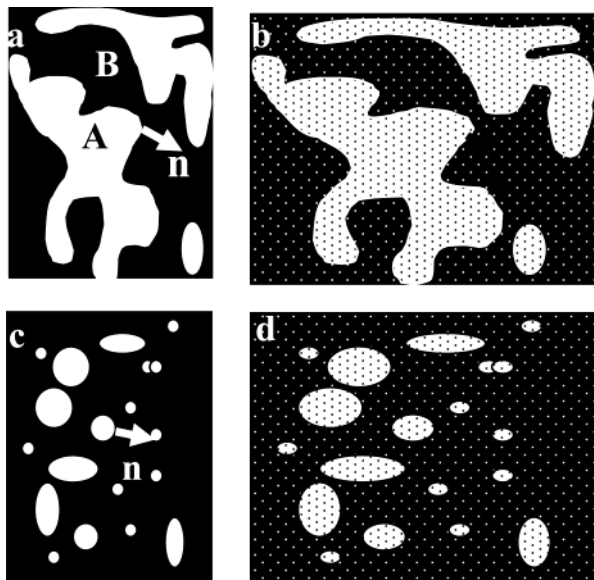


Figure 1. Schematic representation of dry and swollen immiscible polymeric blends, p . (a) and (b) represent co-continuous phases, and (c) and (d) represent a matrix and a dispersed phase. Dots in b and d designate a solvent.

These interfacial variables consist of a scalar and a traceless symmetric second order that describe the local changes of the interfacial size and shape anisotropy densities, respectively.

II. Model Development: A 3D Formulation

Here, we study the behavior of the unsteady isothermal diffusion occurring in a system consisting of a solvent, s , and a two-phase blend, $p = A/B$, of two immiscible polymers, A and B, as shown in Figure 1. The polymeric blend, p , is regarded as a pseudo-one-component system that embeds an interface. We limit our study to the special case where there is no interpenetration between the two components A and B. Such a physical situation may be observed, for instance, far from criticality or in the case of a high friction coefficient between the two immiscible components. In this case, the mass transport process that exclusively occurs in this system is that corresponding to the interpenetration between the solvent and the polymeric blend. Hence, from the two-fluid point of view,¹² the mixture $\{s + p\}$ is regarded as consisting of two interpenetrating media; one is the solvent, s , and the other is the whole polymeric blend, p . Here, our aim is to derive time evolution equations that account for diffusion processes into such complex immiscible systems. Current understandings show that the best step, and also perhaps the most difficult one, to start with in mathematical modeling to provide a proper description of a physical phenomenon, would consist in appropriately determining independent variables singled out to characterize states of the system under consideration. In this formulation, we choose to describe the solvent by ρ_s and \mathbf{u}_s and the polymeric blend by ρ_p and \mathbf{u}_p , denoting the apparent mass and linear momentum field densities, respectively. From the experience gained in rheological and viscoelastic diffusion studies, these hydrodynamic fields (mass and momentum densities) have proven to be insufficient to adequately characterize dynamic behavior of complex media. Indeed, the internal structure couples to diffusion and brings about inertia and viscoelasticity, as it may occur in our system. Since even though its

individual constituents are Newtonian, the polymeric immiscible blend may behave as a viscoelastic structured medium due to the presence of the interface. As the morphology of the interface undergoes changes in its size and shape resulting from the accommodation of the solvent molecules, additional internal structural variables are required. The behavior of the interface may reflect a direct characterization of that of the blend. Consequently, the effects of the internal structural deformations on mass transport are described in this work by tracking the dynamic changes of the interface. The more details we use to describe the interface, the more complete will be our knowledge for discerning its time evolution and dynamic contribution to the diffusion process. However, our aim is to study the diffusion–interface interaction on a level of description that allows us to reasonably follow both the diffusion process and the dynamic changes of the interface. Therefore, we use the two interfacial variables originally introduced in ref 11 and adopted subsequently by several authors^{13–20} to study the flow–interface interaction. These variables are a scalar and a second-order tensor:

$$Q(\mathbf{r}, t) = \int d^2n f(\mathbf{n}, \mathbf{r}, t)$$

$$\mathbf{q}(\mathbf{r}, t) = \int d^2n f(\mathbf{n}, \mathbf{r}, t)(\mathbf{nn} - \frac{1}{3}\mathbf{I}) \quad (1)$$

describing the local changes of the interfacial size and shape anisotropy densities, respectively. \mathbf{n} is the unit vector normal to the interface, and d^2n is the solid angle. \mathbf{I} and \mathbf{nn} are the unit and dyadic second-order tensors, respectively. By definition, $\text{trace}(\mathbf{q}) = 0$. These interfacial variables (1) are defined respectively as the zeroth and second moments of the interfacial kinetic distribution function density $f(\mathbf{n}, \mathbf{r}, t)$.¹¹ Consequently, the set of the independent state variables for the whole mixture $\{s + p\}$ is

$$(\rho, \mathbf{u}, c, \mathbf{J}, Q, \mathbf{q}) \quad (2)$$

where $\rho = \rho_s + \rho_p$ is the global mass density, $\mathbf{u} = \mathbf{u}_s + \mathbf{u}_p$ is the overall momentum density, $c = \rho_s/(\rho_s + \rho_p)$ is the solvent mass fraction, and $\mathbf{J} = (\rho_p/(\rho_s + \rho_p))\mathbf{u}_p - (\rho_s/(\rho_s + \rho_p))\mathbf{u}_s$ is the solvent diffusion mass flux. We have derived governing equations²⁰ for the set (2) describing the structure–flow–diffusion interaction in systems embedding a complex interface. Here, we investigate in more detail the particular case corresponding to the absence of an applied flow

$$\mathbf{u} = \mathbf{0} \quad (3)$$

($\mathbf{u} = \rho \mathbf{v}$, \mathbf{v} is the overall velocity field) and corresponding to the mechanical equilibrium

$$\partial_\alpha p + \partial_\beta \sigma_{\alpha\beta}^{(\text{overall})} = 0 \quad (4)$$

where the scalar $p = -\varphi + \rho(\partial\varphi/\partial\rho) + Q(\partial\varphi/\partial Q) + q_{ij}(\partial\varphi/\partial q_{ij})$ stands for the hydrodynamic pressure and the second-order tensor $\sigma^{(\text{overall})} = \mathbf{JJ}/(\rho c(1 - c)) - \sigma^{(\text{interface})}$ represents the overall extra stress tensor. The quantity $\varphi = \varphi(\rho, c, Q, \mathbf{q})$ refers to the internal free energy density defined as $\Phi = \int d\mathbf{r} (\mathbf{J}^2/(2\rho c(1 - c))) + \int d\mathbf{r} \varphi(\rho, c, Q, \mathbf{q})$, where the first term corresponds to the relative kinetic energy. The Einstein summation convention is used throughout this paper. The symbol $\partial_\alpha(\cdot) \equiv \partial(\cdot)/\partial r_\alpha$ is the spatial derivative of (\cdot) in the α -direction ($\alpha \equiv x, y$, and

z). Moreover, the derivation is based on the requirement of the overall incompressibility

$$\rho = \text{const} \quad (5)$$

Under the constraints (3)–(5), the set of the independent variables (2) reduces to (c, Q, \mathbf{q}) , and the governing equations derived in ref 20 simplify considerably to the following governing equations (6–21) for the study of the interface–diffusion interaction.

The mass conservation of the solvent molecules into the two-phase polymeric blend in the absence of chemical reactions is given by the usual continuity equation

$$\rho \frac{\partial c}{\partial t} = -\partial_\alpha J_\alpha \quad (6)$$

As the dynamic changes of the interface contribute strongly to diffusion, the driving force for mass transport is no longer simply the gradient of the concentration but rather the gradient of the partial derivative of the internal free energy density φ with respect to the mass fraction c , $\partial\varphi/\partial c$. This has been shown for diffusion of solvents into polymeric media,^{10,20} using nonequilibrium considerations.²¹ In this case, the solvent mass flux density in the absence of inertial effects reads as

$$J_\alpha = -\frac{c}{\rho\Lambda_J} \partial_\alpha \left(\frac{\partial\varphi}{\partial c} \right) \quad (7)$$

where Λ_J is a positive phenomenological parameter that is related to the friction coefficient.^{20,22} In the case of interpenetration between two simple fluids (e.g., gases or liquids) or two symmetric polymers with identical mechanical properties, the quantity $\partial\varphi/\partial c$ coincides with the exchange chemical potential. Indeed, in the case of two simple fluids 1 and 2, possessing respectively a chemical potential $\mu_1 = \varphi - c(\partial\varphi/\partial c)$ and $\mu_2 = \varphi + (1-c)(\partial\varphi/\partial c)$, the exchange chemical potential becomes $\mu_2 - \mu_1 = \partial\varphi/\partial c$. Since $\varphi = \varphi(c, Q, \mathbf{q})$, by applying the chain rule to expression 7, i.e., $\partial_\alpha(\partial\varphi/\partial c) = (\partial^2\varphi/\partial c^2)\partial_\alpha c + (\partial^2\varphi/\partial c\partial Q)\partial_\alpha Q + (\partial^2\varphi/\partial c\partial q_{\beta\gamma})\partial_\alpha q_{\beta\gamma}$, and rearranging appropriately the resulting expression, we obtain the following new form for the solvent mass flux density

$$J_\alpha = -\rho D(\partial_\alpha c + A \partial_\alpha Q + E_{\beta\gamma} \partial_\alpha q_{\beta\gamma}) \quad (8)$$

which involves two additional new terms accounting for the local interfacial changes and therefore provides an extended expression for Fick's first law. Furthermore, this expression also includes three functionals: two scalars and one second-order tensor. The first scalar

$$D = \frac{c}{\Lambda_J} \left(\frac{\partial^2\varphi}{\partial c^2} \right) \quad (9)$$

is identified as the diffusivity coefficient, while the second one

$$A = \left(\frac{\partial^2\varphi}{\partial c\partial Q} \right) / \left(\frac{\partial^2\varphi}{\partial c^2} \right) \quad (10)$$

is a new term that couples diffusion to interfacial size changes. The second-order tensor

$$E_{\beta\gamma} = \left(\frac{\partial^2\varphi}{\partial c\partial q_{\beta\gamma}} \right) / \left(\frac{\partial^2\varphi}{\partial c^2} \right) \quad (11)$$

couples diffusion to the anisotropic changes of the interface. These functionals explicitly depend on the concentration as well as on the two structural variables Q and \mathbf{q} . For linear problems such as those corresponding to differential sorption experiments, the quantities D , A , and \mathbf{E} can be approximated by constants. Note that only gradients of the state variables contribute to the mass flux in the absence of an external flow while in its presence²⁰ divergence of stresses may also generate mass transport. Moreover, the third term in (8) involves the third-order tensor $\nabla\mathbf{q}$, which implies the effects of a higher order tensor on mass transport, as opposed to the classical Fickian expression. The combination of eqs 8 and 6 yields

$$\rho \frac{\partial c}{\partial t} = \partial_\alpha (\rho D(\partial_\alpha c + A \partial_\alpha Q + E_{\beta\gamma} \partial_\alpha q_{\beta\gamma})) \quad (12)$$

Clearly, the presence of the two structural variables Q and \mathbf{q} in this continuity equation requires two additional time evolution equations in order to close the set of the governing equations. The time evolution equations for these interfacial variables have already been derived²⁰ and are given by

$$\frac{\partial Q}{\partial t} = \frac{J_\alpha}{\rho(1-c)} \partial_\alpha Q + \left(q_{\alpha\gamma} + \frac{Q}{3} \delta_{\alpha\gamma} \right) d_{\gamma\alpha} - \frac{\Lambda_{qQ}}{\Gamma_0} \left((Q - Q^*) \frac{\partial Q}{\partial t} + (q_{ij} - q_{ij}^*) \frac{\partial q_{ij}}{\partial t} \right) \quad (13)$$

for the interfacial size density and

$$\frac{\partial q_{\alpha\beta}}{\partial t} = \frac{J_\gamma}{\rho(1-c)} \partial_\gamma q_{\alpha\beta} + q_{\alpha\gamma} d_{\gamma\beta} + q_{\beta\gamma} d_{\gamma\alpha} - \frac{q_{\alpha\beta} q_{\theta\gamma}}{Q} d_{\theta\gamma} + \frac{Q}{3} (d_{\alpha\beta} + d_{\beta\alpha}) - \frac{1}{3} \left(q_{\alpha\beta} + \frac{2Q}{3} \delta_{\alpha\beta} \right) d_{\gamma\gamma} - \frac{2}{3} \delta_{\alpha\beta} q_{\theta\gamma} d_{\theta\gamma} - \frac{\Lambda_{qQ}}{\Gamma_0} \left((q_{\alpha\beta} - q_{\alpha\beta}^*) \frac{\partial q_{\alpha\beta}}{\partial t} + \left(\frac{q_{\alpha\beta} q_{ij}}{Q} - \frac{q_{\alpha\beta}^* q_{ij}^*}{Q^*} \right) \frac{\partial q_{ij}}{\partial t} \right) \quad (14)$$

for the interfacial anisotropy density, where

$$d_{\alpha\beta} = (1-H) \partial_\beta \left(\frac{J_\alpha}{\rho(1-c)} \right) \quad (15)$$

represents the rate of strain of the polymeric blend or that of the interface, since $\mathbf{v}_p = -\mathbf{J}/(\rho(1-c))$ represents the velocity vector field. The functional H , to be defined subsequently, is introduced here to ensure the consistency of the interface dynamic with swelling. In eqs 13–15, one substitutes the diffusion mass flux, \mathbf{J} , by its expression 8. In these equations, $\delta_{\alpha\beta}$ is the Kronecker delta symbol, $\Gamma_0 = \Gamma(c=0)$ represents the initial interfacial tension of the dry blend, and Λ_{qQ} is a positive phenomenological parameter having the dimension of the inverse of time and may be related to the relaxation time of the interface, τ_{qQ} , provided that the system can be associated with a characteristic length scale. The latter parameter may also be concentration dependent. The quantities Q^* and \mathbf{q}^* are functionals that provide the local values for the size and shape densities of the interface while ensuring a smooth continuous transition from the initial to the final equilibrium state.

Additional comments about their physical meaning will be provided in the following sections, in particular for the one-dimensional formulation (section IV). Their expressions¹¹ are given by

$$Q^* = \int d^2 n f_0 \frac{(\det \mathbf{F})^2}{|\mathbf{F}^+ \cdot \mathbf{n}|^4} \quad (16)$$

and

$$\mathbf{q}^* = \int d^2 n f_0 \frac{(\det \mathbf{F})^2}{|\mathbf{F}^+ \cdot \mathbf{n}|^4} \left(\mathbf{nn} - \frac{1}{3} \mathbf{I} \right) \quad (17)$$

The quantity f_0 is the initial distribution function related to the initial size density of the interfacial area by $Q_0 = 4\pi f_0$. The second-order tensor \mathbf{F} represents the gradient of the deformation whose components are defined as

$$F_{\alpha\beta} = \frac{\partial r_\alpha}{\partial Y_\beta} \quad (18)$$

where \mathbf{r} and \mathbf{Y} represent the deformed and undeformed coordinate vectors, respectively. Since, in most cases, diffusion is accompanied by swelling of the blend and therefore by an increase in the interfacial size as well as by a rearrangement of the shape, the quantities Q^* and \mathbf{q}^* may show noticeable deviations from their initial values. Such deviations affect not only the behavior of mass transport but also the interface dynamics. The swelling of the polymeric blend can be quantified by the Jacobian of the transformation (18) that gives $V_{\text{deformed}} = V_{\text{undeformed}} \det \mathbf{F}$ measuring the blend volume change. Furthermore, swelling or more generally deformation creates internal stresses within the blend; our model eqs 6–18 are supplemented by the expression for the extra stress tensor

$$\sigma_{\alpha\beta}^{(\text{interface})} = \sigma^{\text{iso}} \delta_{\alpha\beta} + \sigma_{\alpha\beta} \quad (19)$$

where the isotropic contribution²⁰ is

$$\sigma^{\text{iso}} = \frac{2}{3} \left(Q \frac{\partial \varphi}{\partial Q} + 2 q_{ij} \frac{\partial \varphi}{\partial q_{ij}} \right) \quad (20)$$

and the anisotropic term is written as²⁰

$$\sigma_{\alpha\beta} = - \left(2 q_{\alpha\gamma} \frac{\partial \varphi}{\partial q_{\gamma\beta}} + q_{\alpha\beta} \frac{\partial \varphi}{\partial Q} + \frac{2Q}{3} \frac{\partial \varphi}{\partial q_{\alpha\beta}} - \frac{q_{\alpha\beta} q_{\gamma\gamma}}{Q} \frac{\partial \varphi}{\partial q_{\gamma\gamma}} - \frac{2}{3} \delta_{ij} \left(q_{\alpha\beta} + \frac{1}{3} Q \delta_{\alpha\beta} \right) \frac{\partial \varphi}{\partial q_{ij}} \right) \quad (21)$$

The isotropic as well as the anisotropic terms of the stress tensor involve the contribution of both anisotropic parameters ($\propto \partial \varphi / \partial q_{ij}$) as well as that of the interfacial tension ($\partial \varphi / \partial Q = \Gamma(c)$). In expression 20, the first term, also called the Laplace term, is associated with the effects of the interfacial tension ($\propto \Gamma Q$) and the second term is clearly a nonequilibrium correction to the isotropic stresses that is brought about by the anisotropic changes occurring at the interface. This nonequilibrium contribution vanishes when the system reaches its equilibrium state.

III. Internal Free Energy and Thermodynamics

The model (6–21) describes the unsteady diffusion of a solvent into an immiscible polymeric blend and associated with it the dynamic changes of the size and shape of the interface. The governing equations as well as the extra stress tensor are parametrized by the internal free energy density, φ , in which we express all the physical features of the mixture under consideration. The free energy involves two contributions. One is attributed to mixing and a second one to the excess energy attributed to the presence of the interface.

$$\varphi(c, Q, \mathbf{q}) = \varphi^{\text{mixing}}(c) + \varphi^{\text{interface}}(c, Q, \mathbf{q}) \quad (22)$$

In this paper, the mixture is regarded as consisting of two components: one is the solvent, and the other is the two-phase blend. For the sake of simplicity, we have considered the blend as a pseudo-one-component medium whose physical properties are defined as averages of the properties of each of its constituents. This approximation has the advantage of reducing the number of state variables and thus the number of governing equations to be solved. The mixing part of the free energy for the mixture s–p can be well described by the Flory–Huggins mean-field theory.²³

$$\varphi^{\text{mixing}} = \frac{RT}{\Omega_s} (c \ln c + \chi_{sp} c(1 - c)) \quad (23)$$

where R is the gas constant, T is the temperature, and Ω_s is the molar volume of the solvent. In this expression, we have ignored the term $((1 - c) \ln(1 - c)) / x_n$, since x_n representing an average monomer number in the polymer chains is considered to be very large. Here we have used the mass fraction c of the solvent instead of its volume fraction. These two quantities coincide under the incompressibility constraints for both the global mass density ($\rho = \text{const}$) and the material (intrinsic) mass density of the component i ($\gamma_i = m_i / V_i = \rho c_i / \phi_i = \text{const}$, with $c_i = m_i / (m_s + m_p)$ and $\phi_i = V_i / (V_s + V_p)$ representing the mass and volume fractions of $i = s, p$, respectively). As the global mass density can be written as $\rho = \rho_s + \rho_p = \phi \gamma_s + (1 - \phi) \gamma_p$, and the fact that $d\rho = \phi d\gamma_s + (1 - \phi) d\gamma_p + (\gamma_s - \gamma_p) d\phi = 0$, we arrive at $\rho = \gamma_s = \gamma_p$ and therefore at $\phi = c$. The interaction parameter of the solvent/blend mixture can be expressed as an average value of the interaction parameters of the individual systems solvent/component A and solvent/component B, i.e., $\chi_{sp} = \phi_A^* \chi_{sA} + (1 - \phi_A^*) \chi_{sB}$, where $\phi_A^* = V_A / (V_A + V_B)$ is the volume fraction of phase A in blend p \equiv A/B. This is justified by the fact that the polymers A and B are assumed to swell with the same rate and that the molecules of the solvent also move with a same velocity in both phases A and B.

The second term arising in the free energy density expression (22) is attributed to the contribution of the interface and is written as

$$\varphi^{\text{interface}} = (1 - c) \left(\Gamma(c) Q + \frac{1}{2} \alpha_{ijkl}(c) (q_{ij} - q_{ij}^*) (q_{kl} - q_{kl}^*) \right) \quad (24)$$

The first term expresses the effects of the interfacial tension, Γ , between the blend components A and B. The last term introduces the shape anisotropic changes and

is expressed here in a quadratic form involving tensorial quantities. The mathematical justification for this choice comes as a result of a Taylor expansion around equilibrium of the interfacial free energy density: $\varphi^{\text{interface}} = \varphi^* + 1/2\alpha_{ijkl}(q_{ij} - q_{ij}^*)(q_{kl} - q_{kl}^*)$. Therefore, the first term, φ^* , corresponds to the isotropic state and represents the effects of the interfacial tension. The fourth-order tensor appearing in the second term on the right side of eq 24, $\alpha_{ijkl} = (\partial^2\varphi/\partial q_{ij}\partial q_{kl})$, obeys the easily verifiable symmetry properties $\alpha_{ijkl} = \alpha_{klij} = \alpha_{jikl} = \alpha_{ijlk}$. Since the blend is subjected to diffusion, the physical properties of the interface may be affected by its interaction with the solvent molecules as well as by the nature of the diffusion-induced deformation. Consequently, the interfacial tension Γ and the coefficients of the anisotropy tensor α are concentration-dependent.

At equilibrium, the free energy of the system reaches its minimum (i.e., the derivative of the free energy with respect to the state variables must be equal to zero). This criterion might be helpful to distinguish between slow and fast variables. If, in the space of the state variables, the free energy presents for a certain thermodynamic variable, x , an absolute minimum at the equilibrium state (i.e., $\partial\varphi/\partial x = 0$), the variable can be considered as fast. Otherwise, the variable is slow. Applying this criterion to our case, we deduce that the size density Q can therefore be regarded as a slow variable since $\partial\varphi/\partial Q = \Gamma(c)$ which, in most cases, is different from zero. The presence of some surfactants, under certain experimental conditions, may reduce the interfacial tension of the system, i.e., $\Gamma(c) \rightarrow 0$, making the blend more stable from the thermodynamics point of view. On the other hand, from our choice of the internal free energy density for the interface, the anisotropy tensor density, \mathbf{q} , is a fast variable since at the final stage of diffusion $\partial\varphi/\partial q_{ij} = 0$ as $q_{ij} = q_{ij}^*$. Therefore, the quantity \mathbf{q}^* represents the local equilibrium value for the state variable \mathbf{q} . Our problem here needs careful consideration in order to define the equilibrium state for the blend, in particular, for the variables that possess the property of fast variables. Indeed, before the onset of diffusion, the blend occupies an initial state (e.g., dry) that is different from its final swollen equilibrium state (e.g., blend + solvent). Therefore, these two equilibrium states must be expressed into the free energy density. As the transition from the initial state to the final state is mainly produced by diffusion of the solvent, the quantity \mathbf{q}^* is concentration-dependent and is expressed in such a way that the constraint $\partial\varphi/\partial q_{ij} = 0$ is satisfied at both the initial ($c = 0$ within the blend) and final ($c = c_{\text{eq}}$) equilibrium state. One expression for \mathbf{q}^* is that given by eq 17, whose final value $q_{\text{eq}} = q^*(c = c_{\text{eq}})$ is an explicit function of the value of the mass fraction, c_{eq} , at the equilibrium state. The latter is attained when the chemical potential of the simple fluid in the pure state equals its value in the polymeric blend, i.e., $\mu = \mu^0$. The solvent chemical potential is written as

$$\rho(\mu - \mu^0) = \varphi + (1 - c)\frac{\partial\varphi}{\partial c} - Q\frac{\partial\varphi}{\partial Q} - q_{\alpha\beta}\frac{\partial\varphi}{\partial q_{\alpha\beta}} \quad (25)$$

Therefore, at the final equilibrium state ($\mu = \mu^0$ and $(\partial\varphi/\partial q_{\alpha\beta})|_{\text{equilibrium}} = 0$), eq 25 reduces to

$$\varphi + (1 - c)\frac{\partial\varphi}{\partial c} - Q\frac{\partial\varphi}{\partial Q} = 0 \quad (26)$$

Using expressions 21–26, we arrive at the following equation

$$\left(\frac{RT}{\Omega_s}\right)(\ln c_{\text{eq}} + (1 - c_{\text{eq}}) + \chi_{\text{sb}}(1 - c_{\text{eq}})^2) + (1 - c_{\text{eq}})Q_{\text{eq}}\left(-\Gamma\Big|_{c=c_{\text{eq}}} + (1 - c_{\text{eq}})\left(\frac{\partial\Gamma}{\partial c}\right)\Big|_{c=c_{\text{eq}}}\right) = 0 \quad (27)$$

whose solution gives c_{eq} since the other physical parameters are, in principle, experimentally measurable. The quantity $Q_{\text{eq}} = Q^*(c = c_{\text{eq}})$ is the final equilibrium value of the size density.

IV. Diffusion into a Thin Polymeric Blend Consisting of a Matrix and a Dispersed Phase

Many experimental measurements for diffusion such as sorption, permeation, dissolution, or pervaporation are carried out using thin polymeric films. In such situations, the mathematical formulation can be reformulated in a one-dimensional setting. This is justified by the fact that the thickness of the film is very small compared to the dimension of the other directions. In this section, we study diffusion of a solvent into a thin blend of two immiscible polymers constituting a matrix and a dispersed phase. We treat the case where the minor phase consists initially of spherical drops. Let x be the spatial coordinate corresponding to the direction of diffusion. The state variables $c(x, t)$, $Q(x, t)$, and $\mathbf{q}(x, t)$ are functions of one spatial coordinate and time. Because of the particular symmetry of this problem, the anisotropy tensors have the following form

$$\mathbf{q} = \begin{pmatrix} q & 0 & 0 \\ 0 & -q/2 & 0 \\ 0 & 0 & -q/2 \end{pmatrix} \quad \text{and} \quad \mathbf{q}^* = \begin{pmatrix} q^* & 0 & 0 \\ 0 & -q^*/2 & 0 \\ 0 & 0 & -q^*/2 \end{pmatrix} \quad (28)$$

satisfying $\text{tr}(\mathbf{q}) = 0$ and $\text{tr}(\mathbf{q}^*) = 0$. These forms simplify considerably the mathematical formulation. Indeed, the second-order tensor coefficient given by eq 11 becomes

$$\mathbf{E} = \begin{pmatrix} E & 0 & 0 \\ 0 & -2E & 0 \\ 0 & 0 & -2E \end{pmatrix} \quad (29)$$

with $E = (\partial^2\varphi/\partial c\partial q)/(\partial^2\varphi/\partial c^2)$, and the fourth-order tensor appearing in the interface free energy expression 24 becomes

$$\alpha = \begin{pmatrix} \alpha & -2\alpha & -2\alpha & x & x & x \\ -2\alpha & 4\alpha & -2\alpha & x & x & x \\ -2\alpha & -2\alpha & 4\alpha & x & x & x \\ x & x & x & x & x & x \\ x & x & x & x & x & x \\ x & x & x & x & x & x \end{pmatrix} \quad (30)$$

satisfying the symmetry properties given above, where $\alpha = \partial^2\varphi/\partial q^2$. The other components of the matrix (30), denoted by x , do not intervene in the expression of the free energy density due to symmetry considerations, and therefore there is no need for their specification. The corresponding expression in the internal free energy density becomes

$$\alpha_{ijkl}(q_{ij} - q_{ij}^*)(q_{kl} - q_{kl}^*) = 9\alpha(q - q^*)^2 \quad (31)$$

The one-dimensional governing equations are

$$\begin{aligned} \frac{\partial c}{\partial t} &= \frac{\partial}{\partial x} \left(D \frac{\partial c}{\partial x} + A \frac{\partial Q}{\partial x} + 3E \frac{\partial q}{\partial x} \right) \\ \frac{\partial Q}{\partial t} &= - \frac{D}{1-c} \left(\frac{\partial c}{\partial x} + A \frac{\partial Q}{\partial x} + 3E \frac{\partial q}{\partial x} \right) \frac{\partial Q}{\partial x} - (1 - \tilde{Q}^*) \times \\ &\quad \left(q + \frac{Q}{3} \right) \frac{\partial}{\partial x} \left(\frac{D}{1-c} \left(\frac{\partial c}{\partial x} + A \frac{\partial Q}{\partial x} + 3E \frac{\partial q}{\partial x} \right) \right) - \\ &\quad \frac{1}{\tau_{qQ}} \left(\frac{\Gamma(c)}{\Gamma_0} (Q - Q^*) + \frac{27}{2} \frac{\alpha(c)}{\Gamma_0} (q - q^*)^2 \right) \\ \frac{\partial q}{\partial t} &= - \frac{D}{1-c} \left(\frac{\partial c}{\partial x} + A \frac{\partial Q}{\partial x} + 3E \frac{\partial q}{\partial x} \right) \frac{\partial q}{\partial x} - (1 - \tilde{Q}^*) \times \\ &\quad \left(q - \frac{q^2}{Q} + \frac{4Q}{9} \right) \frac{\partial}{\partial x} \left(\frac{D}{1-c} \left(\frac{\partial c}{\partial x} + A \frac{\partial Q}{\partial x} + 3E \frac{\partial q}{\partial x} \right) \right) - \\ &\quad \frac{1}{\tau_{qQ}} \left(\frac{\Gamma(c)}{\Gamma_0} + \frac{27}{2} \frac{\alpha(c)}{\Gamma_0} \left(\frac{q^2}{Q} - \frac{q^{*2}}{Q^*} \right) \right) (q - q^*) \quad (32) \end{aligned}$$

The equations governing the time evolution of the interface include two competing parts. The first one is attributed to the local interfacial changes caused by the solvent mass flux, and the second one is due to relaxation phenomena related to the effects of the interfacial tension and anisotropic changes. Note that the time symmetry is broken during the whole process of diffusion as the dynamic changes of the interface are exclusively caused by dissipative processes as opposed to flow dynamics of complex fluids that are diffusion-free. Therefore, it is interesting to observe that in the case of diffusion the time evolution for the structural variables is governed by a different mathematical structure than that encountered in conventional rheological studies. In the latter and precisely in the nonlinear regime, the time evolution of the internal structure is obtained as a result of both reversible and irreversible competing processes. Here, diffusion is completely irreversible, and the source of irreversibility stems from two distinct dissipative phenomena. Note that the functional H , appearing in eq 15, is replaced, here by $\tilde{Q}^* = Q^*/Q_0$ in such a way that $(1 - \tilde{Q}^*)$ is positive in the case of shrinkage and negative in the case of swelling, where Q_0 being the initial value of the size density of the interfacial area.

The search for solutions of the partial differential equations requires, in addition to the initial condition, the knowledge of boundary conditions. In most complex media, the physics of the boundaries (surface, interface, interphase) is generally different from that of the bulk. Some of the best examples are those related to Marangoni effect observed at the air-liquid interfaces such as in bubbles rising freely in a non-Newtonian fluid or during the airways reopening in lungs. This interfacial effect induced by surface tension gradients is caused by mass exchange of surfactant between the bulk and the surrounding interface. The mass transport between the bulk and the interface, occurring through spontaneous adsorption and desorption processes, creates local inhomogeneities in the interface concentration and therefore leads to a two-dimensional interfacial flow and diffusion. Here, in this study, we deal with two types of interfaces: the interface that is embedded within the immiscible blend and the interface that separates the solvent and the polymeric blend (external

boundary). We have provided an extrinsic study for the embedded interface using a description from the perspective of an observer located outside of the immiscible blend. The interface separating the two immiscible polymers is described by the above-mentioned quantities, i.e., the interfacial size and shape anisotropy densities. Now, we turn our attention to the physics of the interface between the solvent and the immiscible blend that constitutes the boundary condition. In most studies involving partial differential equations, the boundary conditions are set as fixed known values. This assumes that the boundaries reach their equilibrium state in a time scale much faster than that of the bulk. Such a situation may not always hold in complex media where relaxation processes and other physicochemical phenomena may contribute to the dynamics of the boundaries. Indeed, our model involves, in addition to the parabolic equation (32a), two interfacial equations (32b) and (32c) that have a complex mathematical structure including relaxation terms as well as spatial derivative. One notices that the parabolic nature of the classical diffusion equations, such as Fick's or Fourier's equations, attenuates the development of discontinuities. In contrast to that, a special treatment for the boundaries is required when one deals with complex structured media. We need therefore to complete our model equations by deriving equations that directly track the time evolution of the boundaries.

Let $(c_b(t), Q_b(t), q_b(t))$ represent the state variables at the boundaries. As we have already mentioned, we ignore any two-dimensional surface diffusion at the boundaries and consider only the dynamic changes that are produced by the adsorption/desorption processes of the solvent molecules. The governing equation for the solvent mass fraction at the boundary is as

$$\rho_b \frac{\partial c_b}{\partial t} = J_n \quad (33)$$

where ρ_b is the constant surface global mass density and J_n is the solvent mass flux density that is normal to the boundaries and whose expression can be written in the form of a radiation flux

$$J_n = -\rho_b k (c_b - c_{eq}) \quad (34)$$

The multiplication factor, k , representing the adsorption rate is a material constant and depends on the relaxation time of the internal structure. The governing equations for the interfacial variables are

$$\begin{aligned} \frac{\partial Q_b}{\partial t} &= (Q_b - Q_b^*) \frac{J_n}{\rho_b (1 - c_b)} - \\ &\quad \frac{1}{\tau_{qQ}} \left(\frac{\Gamma(c_b)}{\Gamma_0} (Q_b - Q_b^*) + \frac{27}{2} \frac{\alpha(c_b)}{\Gamma_0} (q_b - q_b^*)^2 \right) \\ \frac{\partial q_b}{\partial t} &= (q_b - q_b^*) \frac{J_n}{\rho_b (1 - c_b)} - \\ &\quad \frac{1}{\tau_{qQ}} \left(\frac{\Gamma(c_b)}{\Gamma_0} + \frac{27}{2} \frac{\alpha(c_b)}{\Gamma_0} \left(\frac{q_b^2}{Q_b} - \frac{q_b^{*2}}{Q_b^*} \right) \right) (q_b - q_b^*) \quad (35) \end{aligned}$$

These two equations are written as a sum of two contributions: a relaxation term and an adsorption-induced deformation term. On one hand, the relaxation part is kept similar to that of the bulk because we

assume that the macromolecules located at the boundaries have the same relaxation phenomena as those located in the bulk. Our motivation is justified by the fact that in thin films diffusion can be approximated as a unidirectional process. This might not be true if surface diffusion at the boundaries has to be considered or in the case of a shock-wave-like diffusion observed in glassy polymers. In these cases, the kinetic coefficients (relaxation times) as well as the state equations (surface tension, anisotropy coefficients α) must have different values and/or expressions. On the other hand, the first part of the equations presents a different mathematical structure than those of the bulk, where the net change of the interfacial variables (i.e., $Q - Q^*$, $q - q^*$) is exclusively produced by the adsorption flux. These bulk-effect terms, seen as advection-like phenomena, however produced by diffusion fluxes, drive the interface morphology in the direction of the swelling. The main difference in the mathematical structure between the governing equations of the bulk and those of the boundaries is the absence of the deformation (e.g., swelling) term, $\partial(J/(\rho(1-c)))/\partial x$, that influences the embedded interfacial morphology within the bulk rather than at the boundaries.

As a recapitulation, the model consists of a set of three time evolution partial differential equations for the volume and three time evolution ordinary differential equations for the boundaries that have to be solved simultaneously. The distribution of stresses on the other hand comprises the isotropic component

$$\sigma^{\text{iso}} = \frac{2}{3}(\Gamma Q + 27\alpha(q - q^*)q) \quad (36)$$

and the anisotropic contribution given by

$$\sigma = \begin{pmatrix} \sigma_{11} & 0 & 0 \\ 0 & \sigma_{22} & 0 \\ 0 & 0 & \sigma_{22} \end{pmatrix} \quad (37)$$

where its components are

$$\sigma_{11} = -\Gamma q + 27\alpha\left(\frac{3q^2}{Q} - \frac{4Q}{3}\right)(q - q^*) \quad (38)$$

$$\sigma_{22} = \frac{\Gamma}{2} q + 27\alpha\left(3q + \frac{2Q}{3} - \frac{3q^2}{2Q}\right)(q - q^*) \quad (39)$$

The first normal stress difference is

$$N_1 = -\frac{3}{2}\Gamma q - 27\alpha\left(2Q + 3q - \frac{9q^2}{2Q}\right)(q - q^*) \quad (40)$$

while the second normal stress difference vanishes due to symmetry. All the model equations involve the still analytically undetermined interfacial quantities $Q^*(c)$ and $q^*(c)$. As the thin polymeric blend swells only in the direction of diffusion, the changes are assumed to occur principally in the x -direction. Therefore, the deformation gradient matrix can be written as

$$\mathbf{F} = \begin{pmatrix} F & 0 & 0 \\ 0 & 1 & 0 \\ 0 & 0 & 1 \end{pmatrix} \quad (41)$$

In this one-dimensional setting, we have $F = 1/(1-c)$ since $\det \mathbf{F} = V_{\text{deformed}}/V_{\text{undeformed}}$ and the volume fraction

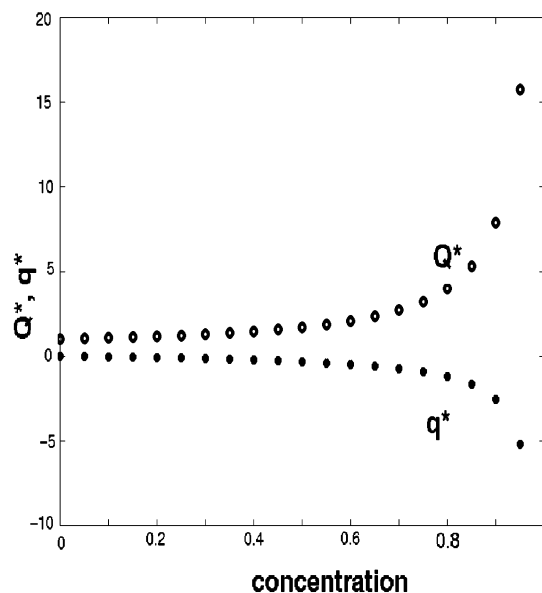


Figure 2. Q^* and q^* vs concentration, c .

coincides with the mass fraction due to the global and material incompressibility constraint as seen in section III. Considering expressions 16 and 17, and using spherical coordinates with $n_x = \cos \theta$, $n_y = \sin \theta \cos \beta$, and $n_z = \sin \theta \sin \beta$ with θ and β being the polar angles, we can write

$$Q^*(c) = \frac{Q_0}{4\pi} \int_0^{2\pi} d\beta \int_0^\pi d\theta \frac{F^2 \sin \theta}{[F^2 \cos^2 \theta + \sin^2 \theta]^2} \quad (42)$$

$$q^*(c) = \frac{Q_0}{4\pi} \int_0^{2\pi} d\beta \int_0^\pi d\theta \frac{F^2 \sin \theta \cos^2 \theta}{[F^2 \cos^2 \theta + \sin^2 \theta]^2} - \frac{1}{3} Q^*(c) \quad (43)$$

where $Q_0 = 4\pi f_0$ is the initial value of the size density for the interfacial area. Integration of eqs 42 and 43 gives

$$Q^*(c) = \frac{Q_0}{2} \left(1 + \frac{F^2}{\sqrt{F^2 - 1}} a \tan \sqrt{F^2 - 1} \right) \quad (44)$$

$$q^*(c) = -\frac{Q_0}{6} \left(\left(\frac{(F^2 - 4)F^2}{(F^2 - 1)^{3/2}} \right) a \tan \sqrt{F^2 - 1} + \left(\frac{F^2 + 2}{F^2 - 1} \right) \right) \quad (45)$$

$F = 1/(1-c) \geq 1$ since the system swells as a result of diffusion. One can verify that at the initial state $Q^*(c=0) = Q_0$ and $q^*(c=0) \approx 0$. The final equilibrium values are given by $Q_{\text{eq}} \equiv Q^*(c=c_{\text{eq}})$ and $q_{\text{eq}} \equiv q^*(c=c_{\text{eq}})$ as shown in Figure 2. Swelling of the blend produces the displacement of the boundaries which requires, numerically, an adjustment of their position during the time of diffusion. One can alternatively solve the governing equations in a fixed frame by reformulating the governing equations in Lagrangian coordinates corresponding to the undeformed polymeric blend. Assuming no overall flow under an overall mechanical equilibrium in a one-dimensional formulation, this task becomes easier and consists of using the mathematical transformation (18) where the Eulerian spatial gradient $\partial/\partial x$ is replaced by Lagrangian spatial gradient $(1/F)(\partial/\partial Y) = (1-c)(\partial/\partial Y)$. In the following, the PDEs are rewritten in Lagrangian coordinates.

V. 1D Dimensionless Equations

The model governing equations are parametrized by a kinetic coefficient (interfacial relaxation time τ_{q0}) and the internal free energy density that involves the solvent and the polymer material parameters. To clarify the relative magnitude of physical interactions, we scale the governing eqs 32–35 to identify dimensionless groups of the model. We use the following dimensionless quantities $X = Y/L_0$ for space and $\theta = t/\tau_d$ for time, where L_0 is the initial thickness of the film, $\tau_d = L_0^2/D_0$ is the diffusion characteristic time scale, and $D_0 = D(c=0)$. The dimensionless quantities for the state variables are $\tilde{c} = c/c_{eq}$, $\tilde{Q} = Q/Q_0$, and $\tilde{q} = q/Q_0$, where c_{eq} is the equilibrium mass fraction and Q_0 is the initial size density that can be measured using X-ray techniques. Under these transformations, the dimensionless governing eqs 32 for the bulk are

$$\begin{aligned} \frac{\partial \tilde{c}}{\partial \theta} &= (1 - c_{eq}\tilde{c}) \frac{\partial}{\partial X} \times \\ &\quad \left((1 - c_{eq}\tilde{c}) \tilde{D} \left(\frac{\partial \tilde{c}}{\partial X} + g_0 \tilde{A} \frac{\partial \tilde{Q}}{\partial X} + 3g_1 \tilde{E} \frac{\partial \tilde{q}}{\partial X} \right) \right) \\ \frac{\partial \tilde{Q}}{\partial \theta} &= -c_{eq}(1 - c_{eq}\tilde{c}) \left(\tilde{D} \left(\frac{\partial \tilde{c}}{\partial X} + g_0 \tilde{A} \frac{\partial \tilde{Q}}{\partial X} + 3g_1 \tilde{E} \frac{\partial \tilde{q}}{\partial X} \right) \frac{\partial \tilde{Q}}{\partial X} + \right. \\ &\quad \left. (1 - \tilde{Q}^*) \left(\tilde{q} + \frac{\tilde{Q}}{3} \right) \frac{\partial}{\partial X} \left(\tilde{D} \left(\frac{\partial \tilde{c}}{\partial X} + g_0 \tilde{A} \frac{\partial \tilde{Q}}{\partial X} + 3g_1 \tilde{E} \frac{\partial \tilde{q}}{\partial X} \right) \right) \right) - \\ &\quad \frac{1}{De} \left(\tilde{\Gamma}(\tilde{Q} - \tilde{Q}^*) + \tilde{\alpha} \left(\frac{27g_1}{2g_0} \right) (\tilde{q} - \tilde{q}^*)^2 \right) \\ \frac{\partial \tilde{q}}{\partial \theta} &= -c_{eq}(1 - c_{eq}\tilde{c}) \left(\tilde{D} \left(\frac{\partial \tilde{c}}{\partial X} + g_0 \tilde{A} \frac{\partial \tilde{Q}}{\partial X} + 3g_1 \tilde{E} \frac{\partial \tilde{q}}{\partial X} \right) \right) \frac{\partial \tilde{q}}{\partial X} + \\ &\quad (1 - \tilde{Q}^*) \left(\tilde{q} - \frac{\tilde{q}^2}{\tilde{Q}} + \frac{4\tilde{Q}}{9} \right) \frac{\partial}{\partial X} \times \\ &\quad \left(\tilde{D} \left(\frac{\partial \tilde{c}}{\partial X} + g_0 \tilde{A} \frac{\partial \tilde{Q}}{\partial X} + 3g_1 \tilde{E} \frac{\partial \tilde{q}}{\partial X} \right) \right) - \\ &\quad \frac{1}{De} \left(\tilde{\Gamma} + \tilde{\alpha} \left(\frac{27g_1}{2g_0} \right) \left(\frac{\tilde{q}^2}{\tilde{Q}} - \frac{\tilde{q}^{*2}}{\tilde{Q}^*} \right) \right) (\tilde{q} - \tilde{q}^*) \quad (46) \end{aligned}$$

and those for the boundaries are

$$\begin{aligned} \frac{\partial \tilde{c}_b}{\partial \theta} &= K(1 - \tilde{c}_b) \\ \frac{\partial \tilde{Q}_b}{\partial \theta} &= K \left(\frac{c_{eq}(1 - \tilde{c}_b)}{1 - c_{eq}\tilde{c}_b} \right) (\tilde{Q}_b - \tilde{Q}_b^*) - \\ &\quad \frac{1}{De} \left(\tilde{\Gamma}(\tilde{Q}_b - \tilde{Q}_b^*) + \tilde{\alpha} \left(\frac{27g_1}{2g_0} \right) (\tilde{q}_b - \tilde{q}_b^*)^2 \right) \\ \frac{\partial \tilde{q}_b}{\partial \theta} &= K \left(\frac{c_{eq}(1 - \tilde{c}_b)}{1 - c_{eq}\tilde{c}_b} \right) (\tilde{q}_b - \tilde{q}_b^*) - \\ &\quad \frac{1}{De} \left(\tilde{\Gamma} + \tilde{\alpha} \left(\frac{27g_1}{2g_0} \right) \left(\frac{\tilde{q}_b^2}{\tilde{Q}_b} - \frac{\tilde{q}_b^{*2}}{\tilde{Q}_b^*} \right) \right) (\tilde{q}_b - \tilde{q}_b^*) \quad (47) \end{aligned}$$

that involve three normalized functionals $\tilde{D}(c, Q, q) = D(c, Q, q)/D_0$, $\tilde{A}(c, Q, q) = (Q_0/c_{eq}g_0)A(c, Q, q)$, and $\tilde{E}(c, Q, q) = (Q_0/c_{eq}g_1)E(c, Q, q)$ and three dimensionless groups

$$g_0 = \frac{\Gamma_0 Q_0 \Omega_s}{RT} \quad g_1 = \frac{\alpha_0 Q_0^2 \Omega_s}{RT} \quad De = \frac{\tau_{q0}}{\tau_d} \quad (48)$$

In addition to these groups, the boundary equations include a fourth parameter $K = L_0^2 k/D_0$ that compares the rate of adsorption to the diffusion time in the bulk. These groups of numbers and the functionals A and E depend explicitly on the physical properties of both the interface and the solvent as well as on the experimental conditions. Moreover, A and E involve the Flory χ parameter expressing the molecular interactions among the constituents of the solvent/blend system. Therefore, the model provides a description of the behavior of diffusion for a particular solvent–blend mixture at a particular experimental condition. While D is chosen to be constant in this study, A and E are functionals that are allowed to explicitly vary with the state variables c , Q , and q . Their expressions are obtained by replacing the internal free energy density (22–24) in eqs 10 and 11. The third dimensionless group De refers to the diffusion Deborah number and compares the diffusion characteristic time scale to the relaxation characteristic time scale of the interface. In this description, it is plausible and justifiable to define the latter, since the blend possesses a characteristic length scale. We recall that the diffusion Deborah number has been introduced^{24,25} to provide a qualitative description of the behavior of mass transport. It is expected that when $De \approx O(1)$, diffusion will exhibit a non-Fickian behavior. In polymeric media, such kinetics has been shown to vary as a power law: t^n where n is an exponent that is equal to $1/2$ for the Fickian behavior, $n = 1$ for the case II mass transport, and $1/2 < n < 1$ for anomalous diffusion. In most general cases, a polynomial expansion $\sum a_n t^n$ is well suitable to fit the experimental data, where a_n is a material parameter. Deviations from the square root kinetics constitute a direct evidence of the occurrence of the non-Fickian character of mass transport produced by viscoelasticity. It is clear that viscoelastic effects are brought about by the presence of the interface and its retarded response. If the interface relaxes slowly in a time scale larger than or comparable to the diffusion characteristic time scale, the dynamic changes of the interfacial variables will be caused by the local changes of the solvent mass fluxes. The local changes of the interfacial variables subsist much longer than in the Fickian case. Consequently, diffusion exhibits a non-Fickian behavior. If, on the other hand, the interface relaxes rapidly to its equilibrium state, the size and anisotropy reach their final values in a time scale much smaller than the time scale of diffusion. In this case, diffusion is Fickian. This qualitative picture can easily be depicted using the qualitative understanding provided by the dimensionless diffusion Deborah number, De , arising in the dimensionless form of the governing equations. Here, we use the following expression $De = D_0 \eta_0 / \Gamma_0 Q_0 L_0^2$, where η_0 is the viscosity of the blend, Γ_0 is the initial interfacial tension, $Q_0 = 3\phi/R_0$, ϕ is the volume fraction of the minor phase in the blend, and R_0 is the radius of the drops. The governing equations are explicitly dependent on the interfacial tension as well as on the anisotropy coefficient α whose expressions require two equations of state. Our choice focuses on the use of the following already existing function of concentration similar to the familiar expressions used for surfactants $\tilde{\Gamma}(\tilde{c}) = \Gamma(\tilde{c})/\Gamma_0 = 1 + \epsilon_{\Gamma} c_{eq} \tilde{c}$ and $\tilde{\alpha}(\tilde{c}) = \alpha(\tilde{c})/\alpha_0 = 1 + \epsilon_{\alpha} c_{eq} \tilde{c}$. In case of shrinkage where the

interfacial area decreases, the interfacial tension decreases with concentration ($\epsilon < 0$), while in case of swelling the interfacial area increases with the concentration ($\epsilon > 0$). In the following, we investigate the case where diffusion is accompanied by swelling, and therefore ϵ is chosen to be positive.

Solutions to the governing eqs 46 and 47 require the knowledge of initial conditions that are

$$\begin{aligned}\tilde{c}(X, \theta=0) &= 0 \\ \tilde{Q}(X, \theta=0) &= 1 \quad \text{for } 0 \leq X \leq 1 \\ \tilde{q}(X, \theta=0) &= 0\end{aligned}\quad (49)$$

Note that this formulation does not require us to impose fixed values for the boundary conditions. Equations 47 constitute the boundary conditions for eqs 46. To solve numerically the governing equations, the model requires, in addition to the initial conditions, the knowledge of the equilibrium state that can be in principle determined from thermodynamics considerations. In sorption experiments, one generally measures the polymer mass uptake during the time of diffusion which is generally used as a good indication to determine the behavior of diffusion and how its kinetics deviates from the Fickian one. The normalized mass uptake is calculated using the following expression:

$$\frac{M(t)}{M_{\text{eq}}} = \int_0^1 \frac{\tilde{c}F}{F_{\text{eq}}} dX \quad (50)$$

As the polymer is assumed to swell only in the direction of diffusion, the normalized deformed thickness of the swollen blend is given by

$$\frac{L(t)}{L_0} = \int_0^1 F dX \quad (51)$$

Similarly, and for practical reasons, we define the net change of the interfacial size density

$$\frac{\Delta Q(t)}{\Delta Q_{\text{eq}}} = \int_0^1 \frac{\tilde{Q} - 1}{\tilde{Q}_{\text{eq}} - 1} \frac{F}{F_{\text{eq}}} dX \quad (52)$$

of the interfacial anisotropy density

$$\frac{\Delta q(t)}{\Delta q_{\text{eq}}} = \int_0^1 \frac{\tilde{q}}{\tilde{q}_{\text{eq}}} \frac{F}{F_{\text{eq}}} dX \quad (53)$$

and of the normalized transient stress tensor components by

$$\frac{\bar{\sigma}(t)}{\Gamma_0 Q_0} = \int_0^1 \frac{\bar{\sigma}}{\Gamma_0 Q_0} \frac{F}{F_{\text{eq}}} dX \quad (54)$$

where $\bar{\sigma} \equiv \sigma_{11}$, σ_{22} , and σ^{iso} .

VI. Numerical Results

In this section, we provide numerical results of the governing eqs 46 and 47. We first study the behavior of mass transport in solvent–blend systems with physical properties similar to those of the model system MeOH–PIB/PDMS. The polymeric blend of a 1 mm thickness has an interfacial tension $\Gamma_0 = 2.3 \times 10^{-3}$ N/m, a size density $Q_0 = 2.6 \times 10^6$ m⁻¹, a viscosity $\eta_0 = 100$ Pa s, and an anisotropy coefficient $\alpha = 3 \times 10^{-11}$ N. The solvent has a molar volume $\Omega_s = 4.05 \times 10^{-5}$ m³/mol

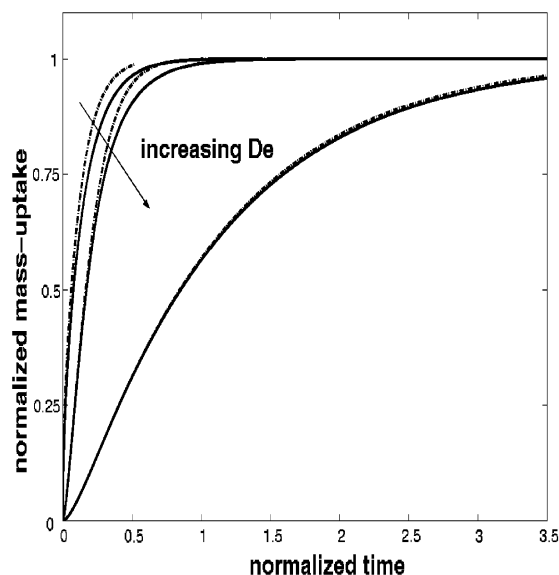


Figure 3. Polymer mass uptake vs normalized time for $De = 10^{-5}$, 0.1, and 1. Solid lines correspond to $g_0 = 0.9$ and dashed lines to $g_0 = 10^{-4}$.

and a diffusivity coefficient $D_0 = 10^{-11}$ m²/s. The equilibrium mass fraction is chosen to be 0.1, which gives, using expressions 44 and 45, the interfacial equilibrium values of $Q_{\text{eq}}/Q_0 = 1.0748$ and $q_{\text{eq}}/Q_0 = -0.0392$ for the size and anisotropy densities, respectively. The Deborah number is of the order of 10^{-5} , leading to a fast relaxation of the interface to its final swollen state. The coupling constants appearing in the dimensionless time evolution equations are $g_0 = 10^{-4}$ and $g_1 = 3.7 \times 10^{-6}$, demonstrating a weak coupling between diffusion and the dynamic changes of the interface morphology. In this case, diffusion mainly influences the time evolution of the interfacial variables through the concentration gradients. Therefore, one expects to observe a Fickian behavior. A clear indication of this result is confirmed by the blend mass-uptake curve vs normalized time given in Figure 3, which shows the usual Fickian time square root function (i.e., first curve starting from the left). We also study the effect of Deborah number for fixed values of the coupling constant g_0 as well as that of the coupling constant g_1 for fixed values of De . In the following, by requiring more symmetry for the dissipation part at the initial state, we arrive at the constraint $(q - q^*)\partial\varphi/\partial Q = 3Q \partial\varphi/\partial q$ that gives $g_1 = g_0/27$. The constant k in expression 34 is chosen to be equal to k_1/τ_{Qq} . The proportionality to the relaxation time inverse of the interface is justified from previous experimental results.²⁶ The multiplication factor k_1 is set here by numerical trial and error to be equal to 0.1. More physical insight is needed here to define quantitatively the parameters entering the expression of the adsorption mass flux.

Figure 3 also shows the profiles of mass uptake vs time for three different values of $De = 10^{-5}$, 0.1, and 1 for $g_0 = 10^{-4}$ (dashed lines) and $g_0 = 0.9$ (solid lines). The effects of g_0 on the kinetics of diffusion are noticeable for small values of De . For relatively larger values than those leading to the Fickian regime, the slow relaxation of the interfacial variables dominates during the process of mass transport, and the process becomes a relaxation-controlled rather than diffusion-controlled. This may be understood from the fact that the coupling constants g_0 and g_1 intervene directly in the speed of the advancing solvent fronts within the polymeric blend.

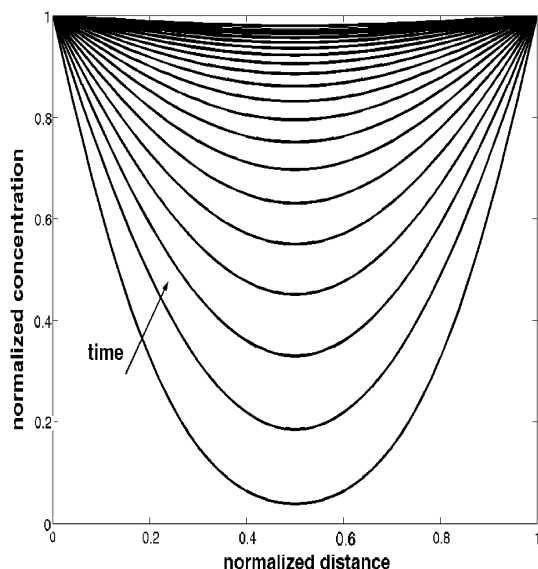


Figure 4. Profiles of concentration, \hat{c} , against normalized thickness of the blend for $De = 10^{-5}$ and $g_0 = 10^{-4}$ (normalized time step = 1.2×10^{-2}).

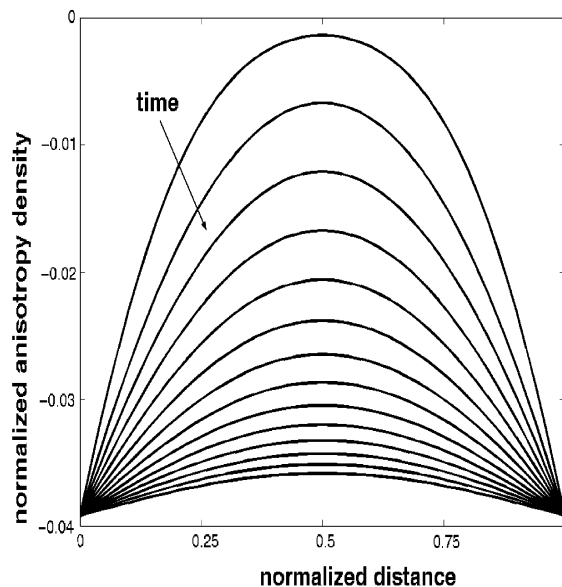


Figure 6. Profiles of normalized anisotropy density, \hat{q} , against normalized thickness of the blend for $De = 10^{-5}$ and $g_0 = 10^{-4}$ (normalized time step = 1.2×10^{-2}).

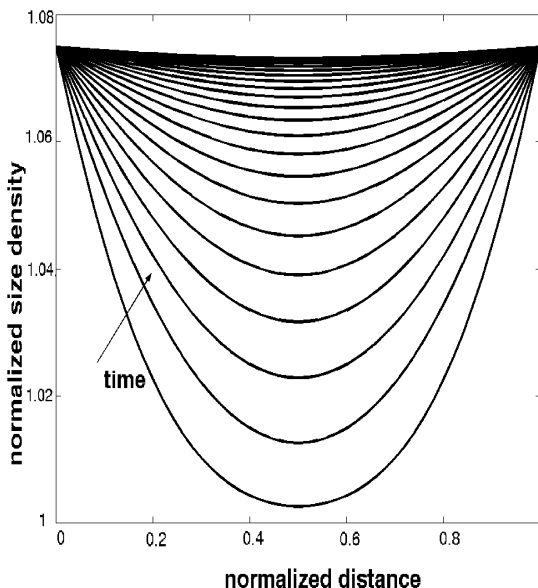


Figure 5. Profiles of normalized size density, \hat{Q} , against normalized thickness of the blend for $De = 10^{-5}$ and $g_0 = 10^{-4}$ (normalized time step = 1.2×10^{-2}).

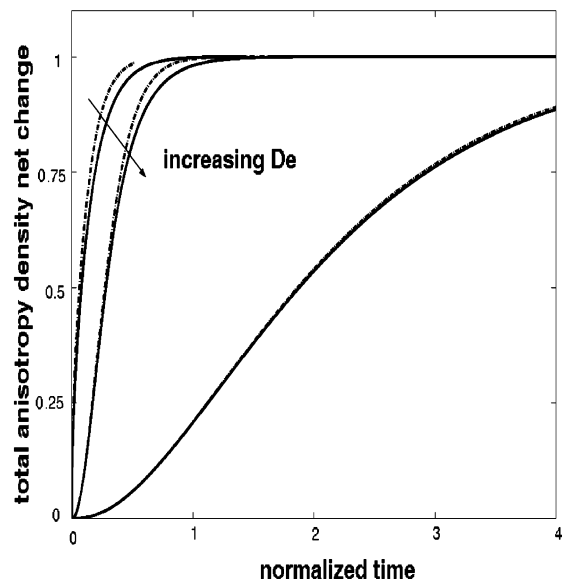


Figure 7. Time evolution of the net change of the total anisotropy density for $De = 10^{-5}$, 0.1, and 1. Solid lines correspond to $g_0 = 0.9$ and dashed lines to $g_0 = 10^{-4}$.

Generally, clear deviations from Fickian diffusion are observed when De approaches unity.

Figure 4 shows the profiles of concentration vs normalized thickness of the blend for $g_0 = 10^{-4}$ and $De = 10^{-5}$. As expected, these profiles are typically Fickian, where the gradients of concentration become the dominant driving force generating mass fluxes. The calculated profiles can be recovered as classical solutions of the parabolic diffusion equation. In this case, the relaxation of the interface is faster than the motion of the solvent molecules that do not have time to notice any dynamic changes occurring at the interface.

The same tendency is also observed for the interfacial variables Q and q as shown respectively in Figures 5 and 6. As discussed earlier, diffusion, mainly produced by the gradients of concentration for small values of g_0 , influences unilaterally the evolution of the interface. The effects of coupling between diffusion and the interface deformation are much weaker on the side of

diffusion than on the side of the interface dynamics. For small values of De , the fast relaxation phenomenon predominates during the time evolution of the interface whose behavior mainly exhibit a Fickian-like character. Indeed, the relaxation parts of the interface governing equations are strong functions of the concentration, via the functionals Q^* and q^* . For larger values of De , gradients of concentration become the driving forces for the dynamic changes of the interface.

Note that the study of the dynamics of the interface may provide an interesting and alternative framework to track the behavior of diffusion and vice versa. The net change of the anisotropy density follows the square root kinetics for $g_0 = 10^{-4}$ and $De = 10^{-5}$ as shown in Figure 7. As in the case of the blend mass uptake, the net change of the interfacial anisotropy density also exhibits a behavior that does not follow the square root kinetics for De approaching unity. Moreover, the inter-

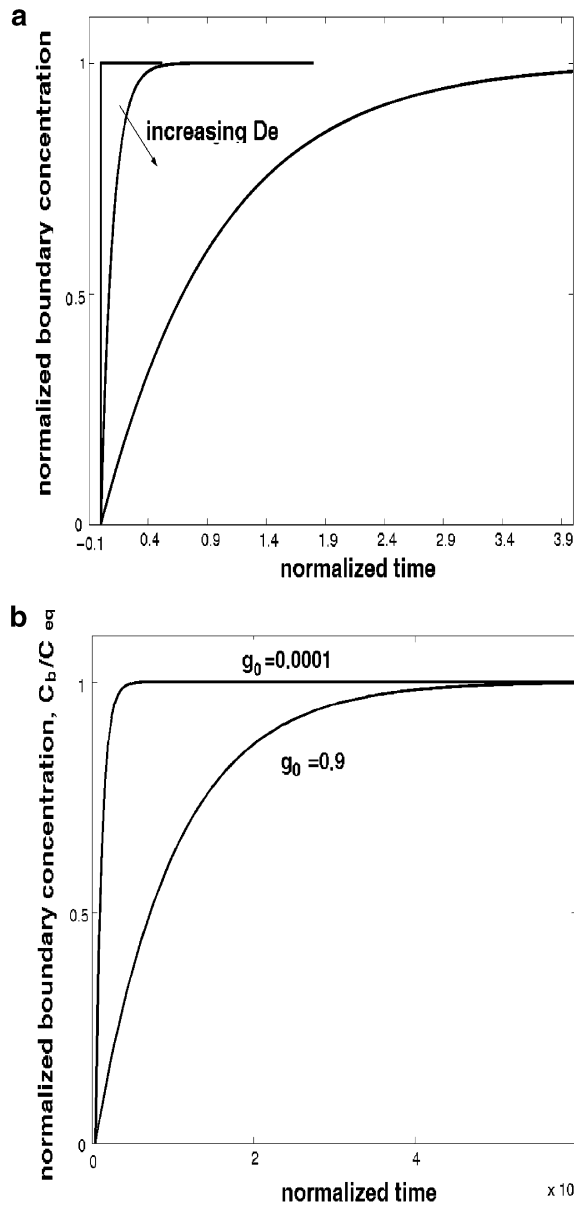


Figure 8. (a) Time evolution of the normalized concentration at the boundary, \bar{c}_b , for $De = 10^{-5}$, 0.1, and 1. (b) Time evolution of the normalized concentration at the boundary, \bar{c}_b , for $De = 10^{-5}$.

facial variables show a slow evolution compared to that followed by the blend weight gain, in particular at the initial stages of the sorption process.

We have observed that the behavior of mass transport as well as that of the dynamic changes of the interface is strongly influenced by the time evolution of the boundaries. The profiles of the mass fraction, the size, and the anisotropy densities at the boundaries are shown in Figures 8a,b, 9, and 10, respectively, for different values of the De . For large values of De , diffusion becomes an adsorption-controlled process at the boundaries.

The behavior at the boundaries for the adsorption process is, without big surprises, Fickian-like. Only the rate, at which the equilibrium is reached, changes as De increases. This is attributed to our choice of the adsorption rate, k , to be inversely proportional to the relaxation time of the interface. The effects of g_0 on the time evolution of the boundaries are only seen for very small values of De , as shown in Figure 8b. The plateau

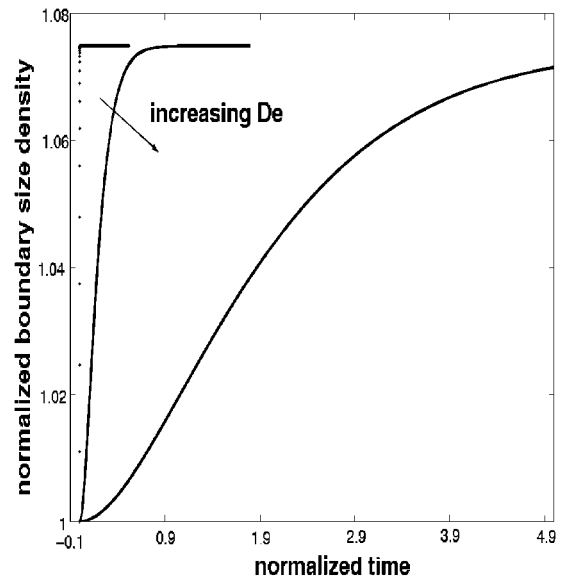


Figure 9. Time evolution of the normalized size density, \bar{Q}_b , at the boundary for $De = 1$, 0.1, and 10^{-5} .

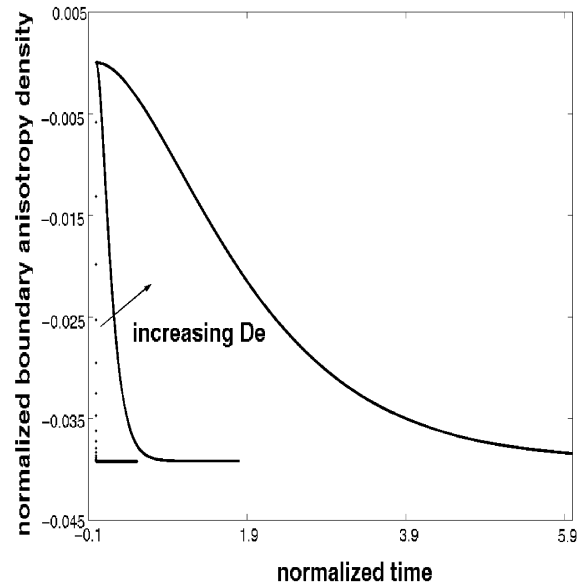


Figure 10. Time evolution of the normalized anisotropy density, \bar{q}_b , at the boundary for $De = 10^{-5}$, 0.1, and 1.

is reached faster for a weak coupling. No such effects have been detected for large De as shown in Figure 8a.

Figure 9 shows the profiles of the size density, \bar{Q}_b , vs normalized time for different values of De . As opposed to the evolution of the concentration at the boundaries, the effects of competing processes between the adsorption and the relaxation phenomena are visible on the time evolution. The profiles can no longer be reproduced by the usual time square root function for larger De . This is more obvious for $De = 1$, where we observe an induction time at the initial stage of the adsorption process.

Figure 10 shows the profiles of the anisotropy density, \bar{q}_b , vs normalized time for different values of De . Even though the anisotropy density is regarded as a fast variable, its time evolution is a result of direct processes as well as of indirect processes due to its intimate coupling with the time evolution of the size density. This

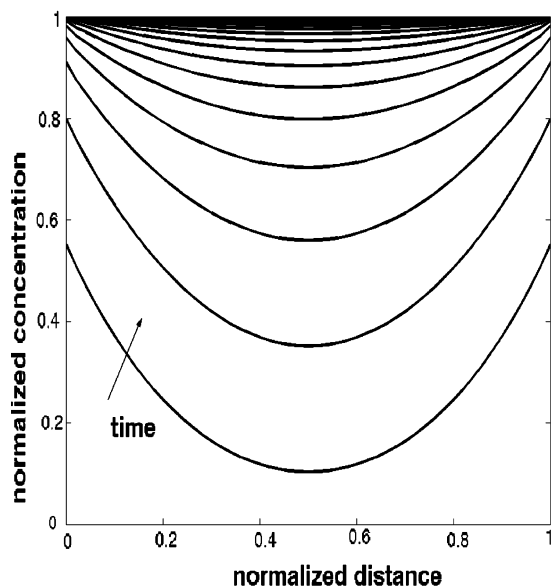


Figure 11. Normalized concentration profiles against normalized thickness of the blend for $g_0 = 0.9$ and $De = 0.1$ (normalized time step = 8×10^{-2}).

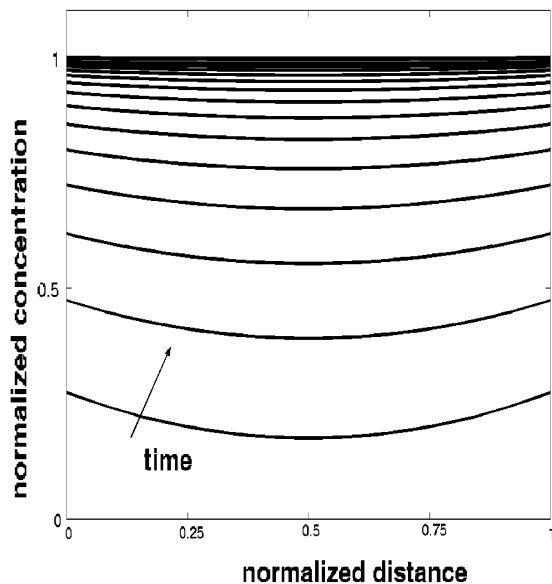


Figure 12. Normalized concentration profiles against normalized thickness of the blend for $g_0 = 0.9$ and $De = 1$ (normalized time step = 0.16).

explains the resemblance of the profiles in this figure with those of Figure 9. However, at the swollen equilibrium state, the internal free energy becomes minimum with respect to q while it is not with respect to the interfacial size density Q .

Figures 11 and 12 show the profiles of concentration vs normalized distance for $De = 0.1$ and 1. The more we increase De , the more the gradients of concentration become insignificant within the polymeric blend. This is also observed for the interfacial variables Q and q (not shown here). In this case, no process is prevailing, and the driving force for mass transport is produced by simultaneous and local changes created by the gradients of the three variables c , Q , and q .

Diffusion in polymeric blends is generally accompanied by swelling that creates internal stresses. Time evolution of the distributions of such stresses is calcu-

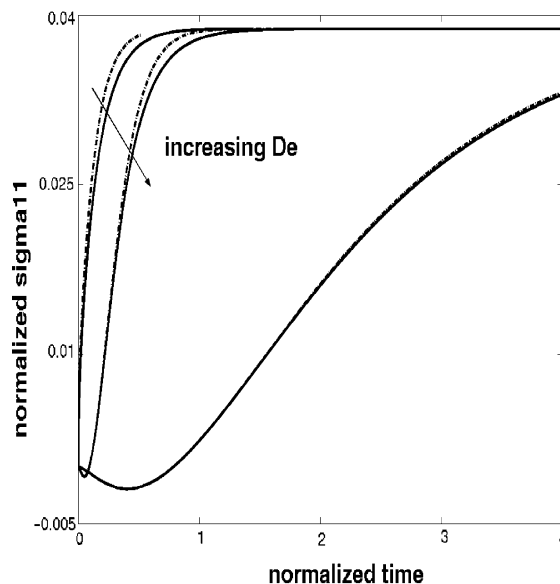


Figure 13. Normalized first component of the stress tensor, $\tilde{\sigma}_{11}$, vs normalized time for $De = 10^{-5}$, 0.1, and 1. Solid line correspond to $g_0 = 0.9$ and dashed lines to $g_0 = 10^{-4}$.

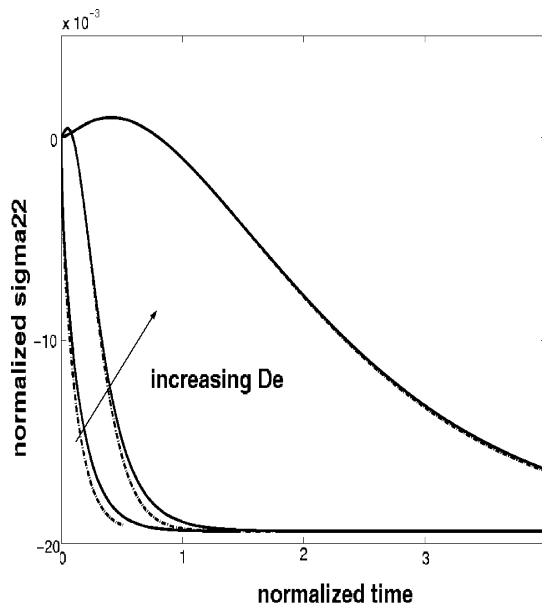


Figure 14. Normalized second component of the stress tensor, $\tilde{\sigma}_{22}$, vs normalized time for $De = 10^{-5}$, 0.1, and 1. Solid line correspond to $g_0 = 0.9$ and dashed lines to $g_0 = 10^{-4}$.

lated using eq 54 and are shown in Figures 13–15. The normalized first component, $\tilde{\sigma}_{11}$, of the anisotropic extra stress tensor exhibits an undershoot that becomes more pronounced when De approaches the unity (Figure 13).

On the other hand, the normalized second component, $\tilde{\sigma}_{22}$, shows an overshoot (Figure 14). No such effects are detected for the isotropic contribution, $\tilde{\sigma}^{iso}$ to the stress tensor (Figure 15). Contrary to the positive values of $\tilde{\sigma}_{11}$ expressing the blend swelling, the negative values of $\tilde{\sigma}_{22}$ show that the shape is subjected to compressing forces in the directions normal to diffusion. However, the shape of the drops is not expected to deform in such directions since swelling forces oppose such changes. What is interesting to note is that the first normal stress difference is different from zero, demonstrating the viscoelastic behavior of diffusion. On the other hand, the second normal stress difference vanishes by sym-

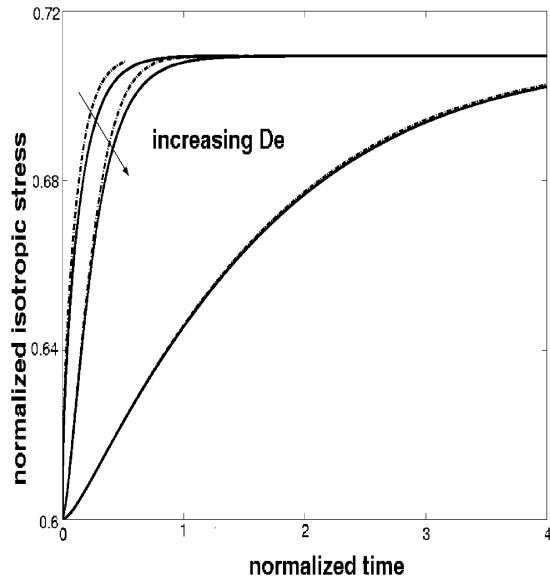


Figure 15. Normalized isotropic stress tensor, $\bar{\sigma}^{\text{iso}}$, vs normalized time for $De = 1, 0.1,$ and 10^{-5} . Solid line correspond to $g_0 = 0.9$ and dashed lines to $g_0 = 10^{-4}$.

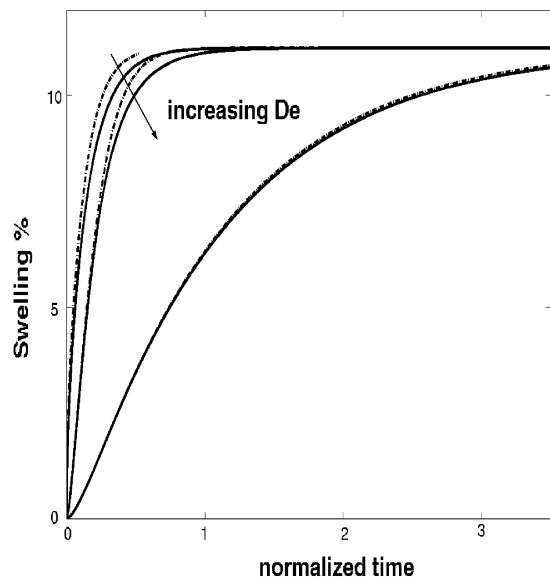


Figure 16. Swelling of the blend vs normalized time for $De = 10^{-5}, 0.1,$ and 1 . Solid line correspond to $g_0 = 0.9$ and dashed lines to $g_0 = 10^{-4}$.

metry. An interesting behavior is expected to occur for a dispersed phase consisting of drops with an initially complex shape. As discussed earlier, the coupling constants g_0 and g_1 affect the time evolution of stresses for small De . The plateau is reached more or less rapidly depending on the values of De .

Figure 16 shows the macroscopic swelling of the blend vs the normalized time for different values of De . These profiles are calculated using eq 51, where the gradient of the deformation, F , in the direction of diffusion depends explicitly on the concentration of the penetrants and therefore implicitly on the interfacial variables Q and q . The same reasoning that has been discussed previously concerning the kinetics of mass uptake applies here as well for the kinetics of swelling.

The global macroscopic swelling of the blend is a result of internal changes of the internal structure that affects the shape of the interface. Initially, the dispersed phase consists of spherical drops that are expected to

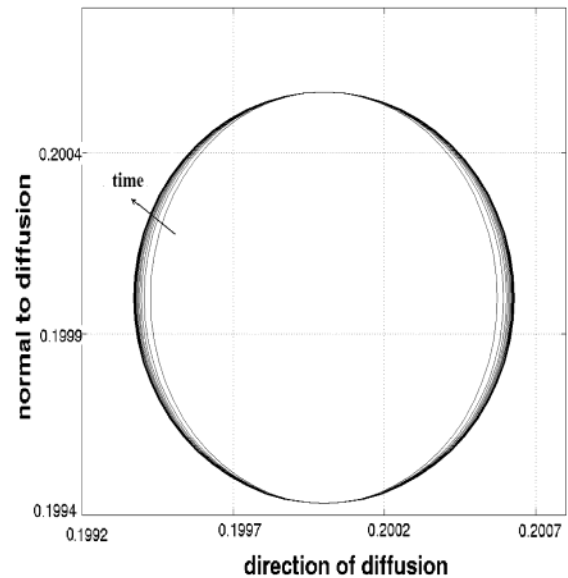


Figure 17. Time evolution of the shape of a drop for $De = 10^{-5}$ and $g_0 = 10^{-4}$.

become, in subsequent times, ellipsoids due to the particular geometry and symmetry of the system. The time evolution of the shape is calculated using the equation

$$\left(\frac{x(t) - x_0}{F(t)R_0}\right)^2 + \left(\frac{y - y_0}{R_0}\right)^2 + \left(\frac{z - z_0}{R_0}\right)^2 = 1$$

where R_0 is the initial radius of the drops and $F(c(x,t))$ is the component of the gradient of deformation defined above. The vector $(x(t), y(t), z(t))$ represents the time-dependent deformed position coordinate of the shape of a drop located at (x_0, y_0, z_0) . Figure 17 shows the time evolution of a drop of radius $R_0 = 5.6 \times 10^{-7}$ m initially located at the position $(2 \times 10^{-4} \text{ m}, 2 \times 10^{-4} \text{ m}, 2 \times 10^{-4} \text{ m})$ within a blend of thickness 10^{-3} m. The dimensionless parameters used in this simulation are $De = 10^{-5}$, $g_0 = 10^{-5}$, and $g_1 = 3.7 \times 10^{-6}$ and correspond to the MeOH-PIB/PDMS mixture. We show the projection of the ellipsoids in the (x, y) plan, since the y and z directions are symmetric by any rotation around the x axis corresponding to the diffusion direction.

VII. Conclusion

We have derived a 3D model to investigate the behavior of mass transport of a solvent into an immiscible polymeric blend. The model consists of a set of coupled nonlinear equations governing the time evolution of the solvent mass fraction and two structural variables accounting for the local dynamic changes of the interface morphology, namely the interfacial size and shape anisotropy densities. An expression for the distribution of stresses created by diffusion is also provided. The model is parametrized by the free energy density in which we express the physics of the system under consideration. We suggest an extended form for the excess energy arising from the presence of the interface. This expression includes the well-known term attributed to the effects of the interfacial tension and a new term expressing the contribution of the shape anisotropy of the interface. Since diffusion is generally accompanied by swelling, we express the governing

equations in Lagrangian coordinates. We investigate in more detail the case corresponding to a 1D diffusion process in a thin polymeric blend consisting of a matrix and a dispersed phase. The physics of the boundaries is further discussed by deriving governing equations to follow their time evolution. Three dimensionless groups of physical parameters emerge naturally in the dimensionless formulation: two constants couple diffusion to the dynamic changes of the interface, and one is the diffusion Deborah number that compares the diffusion characteristic time to the interface relaxation time. Numerical results for a blend consisting of two immiscible Newtonian polymers with physical properties similar to those of the model blend PIB/PDMS predict a typically Fickian behavior. By varying the Deborah number, we were able to cover and predict a wide range of non-Fickian behavior. The coupling constants slightly influence mass transport when De approaches unity. Mass transport becomes viscoelastic in that case. This is expected, since viscoelasticity is brought about by the dynamic changes of the interface and its relaxation rate. The Deborah number dictates the behavior of mass transport as well as that of the dynamic changes of the interface.

This study opens new possibilities for experimental investigations of diffusion into immiscible polymeric blends.

Acknowledgment. Financial support provided by the U.S. Department of Energy (Award DE-FG02-01ER63119) is gratefully acknowledged. D. P. Gaver III acknowledges support through NASA Grant NAG-3-2734. D. De Kee also acknowledges support through NASA Grants NAG-1-02070 and NCC3-946.

References and Notes

(1) Alfrey, T.; Gurnee, E. F.; Lloyd, W. G. *J. Polym. Sci., Part C* **1966**, *12*, 249–261.

- (2) Beris, A.; Edwards, B. *Thermodynamics of Flowing Systems*; Oxford University Press: New York, 1994.
- (3) Thomas, N. L.; Windle, A. H. *Polymer* **1978**, *19*, 255–265.
- (4) Neogi, P. *AIChE J.* **1983**, *29*, 829–839.
- (5) Durning, J. C.; Tabor, M. *Macromolecules* **1986**, *19*, 2220–2232.
- (6) Kalospiros, N. S.; Ocone, R.; Astarita, G.; Meldon, J. H. *Ind. Eng. Chem. Res.* **1991**, *30*, 851–864.
- (7) Wu, J. C.; Peppas, N. A. *J. Appl. Polym. Sci.* **1993**, *49*, 1845–1856.
- (8) Billovits, G. F.; Durning, C. J. *Macromolecules* **1993**, *26*, 6927–6936.
- (9) Edwards, D.; Cohen, D. S. *AIChE J.* **1995**, *41*, 11, 2345–2355.
- (10) El Afif, A.; Grmela, M. *J. Rheol.* **2002**, *46*, 591–628.
- (11) Doi, M.; Ohta, T. *J. Chem. Phys.* **1991**, *95*, 1242–1948.
- (12) De Gennes, P. G. *Macromolecules* **1976**, *9*, 587–593.
- (13) Lee, H. M.; Park, O. O. *J. Rheol.* **1994**, *38*, 1405–1425.
- (14) Grmela, M.; Ait Kadi, A. *J. Non-Newtonian Fluid Mech.* **1994**, *55*, 191–199.
- (15) Grmela, M.; Ait Kadi, A.; Utracki, L. A. *J. Non-Newtonian Fluid Mech.* **1998**, *77*, 253–259.
- (16) Wetzal, E. D.; Tucker, C. L., III. *Int. J. Multiphase Flow* **1999**, *25*, 35–65.
- (17) Wagner, N. J.; Öttinger, H. C.; Edwards, B. J. *AIChE J.* **1999**, *45*, 1169–1181.
- (18) Lacroix, C.; Grmela, M.; Carreau, P. J. *J. Rheol.* **1998**, *42*, 41–62.
- (19) Almusallam, A. S.; Larson, R. G.; Solomon, M. J. *J. Rheol.* **2000**, *44*, 1055–1083.
- (20) El Afif, A.; De Kee, D.; Cortez, R.; Gaver, D. P. I., III and II. *J. Chem. Phys.* **118** (June 2003).
- (21) Grmela, M.; Oettinger, H. C. *Phys. Rev. E* **1997**, *56*, 6620–6632. Oettinger, H. C.; Grmela, M. *Phys. Rev. E* **1997**, *56*, 6633–6655.
- (22) Bearman, R. J. *J. Phys. Chem.* **1961**, *65*, 1961–1968.
- (23) Flory, P. *Principle of Polymer Chemistry*; Cornell University Press: Ithaca, NY, 1953.
- (24) Vrentas, J. S.; Jarzelski, C. M.; Duda, J. L. *AIChE J.* **1975**, *21*, 894–901.
- (25) Vrentas, J. S.; Duda, J. L. *J. Polym. Sci., Polym. Phys. Ed.* **1977**, *15*, 441–453.
- (26) Long, F. A.; Richman, D. *J. Am. Chem. Soc.* **1960**, *82*, 513–519.

MA0342271